USING EXPERIMENTAL AND NUMERICAL CHARACTERIZATION IN COMPARING MARINE EXHAUST SYSTEM STAINLESS STEELS

GORAN VUKELIC[1], JOSIP BRNIC[2]

[1] University of Rijeka, Faculty of Maritime Studies
Studentska 2, Rijeka, Croatia
gvukelic@pfri.hr, www.pfri.uniri.hr

[2] University of Rijeka, Faculty of Engineering
Vukovarska 58, Rijeka, Croatia
brnic@riteh.hr, www.riteh.uniri.hr

Key words: Stainless steel, Material selection, Material characterization.

Abstract. Material selection is one of the crucial points of mechanical design process. Selecting proper material is even more important when designing a component that is going to be exposed to harsh operating conditions like in the marine environment. This paper presents a comparison of three different austenitic stainless steels (1.4541, 1.4571, 1.4841) used in a production of marine exhaust systems. Selecting a suitable material can help in avoiding failure scenarios of such systems that are exposed to elevated temperatures and marine environment. Steels are compared based on experimentally and numerically determined properties and characteristics. Experimentally, ultimate tensile strength and yield strength are determined at room and elevated (300 °C, 600 °C) temperatures. Also, a short-term creep test is performed in order to compare material creep responses for selected temperatures. Further, Charpy impact energy is experimentally measured and value of fracture toughness calculated. As for the numerical research, finite element (FE) simulation of Charpy test is performed. Also, in order to predict fracture behaviour of considered steels, single specimen test method used in fracture mechanics is numerically simulated. Using FE stress analysis results of such test, *J*-integral is calculated to quantify crack driving force. This numerical research was performed in order to establish reliable models that can be used in industry to characterize materials, opposite to traditional experiments, and has proven to be reasonably accurate and efficient. Comparing the results obtained by experimental and numerical assessment of the three considered stainless steels, it can be noted that 1.4841 has the highest yield and ultimate tensile strength along with Charpy impact energy and fracture toughness. Also, steel 1.4841 has higher values of *J*-integral, making it more adequate to structures that need less susceptibility to fracture. Numerically predicted values comply with those experimentally determined ensuring further use of the FE models. Results can be useful in a design process when selection of proper material is of a great importance.

1 INTRODUCTION

Traditional approach to structural design and material selection suggests that anticipated design stress is to be compared to flow properties of considered material. On the other hand,

fracture mechanics approach quantifies flaw size, material fracture toughness and applied stress. In order to have thorough insight into the material behaviour and potential structural failures, designers need to perform calculations using both approaches [1].

Adequate selection of material is a step of a great importance in the design process, otherwise product profitability may be affected, service lifetime reduced and flaws resulting in failures can be expected. Several requirements have to be met during material selection process, such as adequate strength of material, acceptable rigidity level, resistance to elevated temperatures, sufficient resistance to crack propagation.

Stainless steels are general choice when designed structures and constructions need to be corrosion resistant in a specific environment, but also have to withstand high stresses, excessive temperatures or have to be able to operate in specific conditions retaining their functionality [2] (food, nuclear or petrochemical industry, marine environment, surgery or implanting, etc.). So, besides knowing their common mechanical properties like yield strength or maximum tensile strength, description of fracture behaviour is also welcome.

Several examples of stainless steel construction failures and researches on the topic of improving understanding of stainless steels mechanical behaviour are brought to attention here. Recent research proved that integrity of asymmetric double cracked stainless steel pipes subjected to combined tension and bending can be evaluated using the theoretical plastic collapse stress of the single notched pipe [3]. In order to account for creep rupture, basic modelling of phenomena in austenitic stainless steels was performed showing that predicted rupture times for ductile rupture are longer than those for brittle rupture at high stresses and low temperatures with a reversed situation at low stresses and high temperatures [4]. Overpressure in refinery stainless steel pipes was studied to determine material behaviour that led to microstructural change of material and final plastic collapse of pipes [5]. Finite element analyses were performed to gain insight into the failure mechanism of high strength stainless steel bridge roller bearings proving that service loading coupled with wedge imperfection was sufficient for final failure [6]. Although considered as resistant to corrosion, stainless steels can still suffer from corrosion induced failures in specific conditions, like the example of failed handrail [7]. Austenitic stainless steel pipelines used as a conduit for gaseous nitrogen failed due to stress-corrosion cracking caused by synergistic effect of chloride ions, thermal stresses from welding and the presence of sensitized grains of the material [8].

Characterization of material is essential to perform adequate material selection and it is usually done using experimental routines [9] that can be complemented, if not substituted, with numerical prediction of material properties [10, 11] using modern numerical analysis [12] routines backed with powerful computer processors.

Research presented in this paper is a comparison of mechanical properties and fracture behaviour of three austenitic stainless steels, 1.4541, 1.4571 and 1.4841. Ultimate tensile strength, yield strength and Charpy impact energy are experimentally determined for considered steels. Fracture behaviour is compared using numerically calculated J-integral values. Experimentally and numerically obtained results are compared and discussed with a conclusion given on material properties and characteristics.

2 MATERIALS AND METHODS

Three materials are compared: steels 1.4541, 1.4571 and 1.4841. These are austenitic

chromium-nickel alloys. Austenitic stainless steels are the most common stainless steels and are used for building and construction, consumer products, industrial applications. They are generally non-magnetic, easy to form, weld, repair and aesthetically finish.

1.4541 is similar to 1.4301, but with addition of titanium that reduces or prevents carbide precipitation during welding and in elevated temperature service. It possesses good creep strength and is typical used in high-temperature tempering equipment, heavy duty exhaust systems, boilers and welded pressure vessels, oil refinery equipment.

1.4571 contains titanium that stabilizes the structure of material at temperatures over 800°C. This prevents carbide precipitation at the grain boundaries so 1.4571 can be exposed to higher temperatures for a longer period without sensitization. It can be used for furnace parts, chemical equipment, heat exchangers, jet engine parts and structures exposed to marine environment.

1.4841 has excellent high-temperature resistance characteristics when compared with the rest of the austenitic stainless steels series, however if exposed to elevated temperatures for prolonged period it can become very brittle. Added silicon improves oxidation and carburization resistance. It is used in radiant tubes, annealing and carburizing boxes, furnace equipment and heat treatment components.

Mechanical properties of the steels were determined on a computer directed materials testing machine Zwick/Roell, 400 kN, using specimens manufactured from rods of considered steels. Appropriate ASTM standard was used to set specimen geometry and uniaxial tensile test procedure [14], Fig. 1.
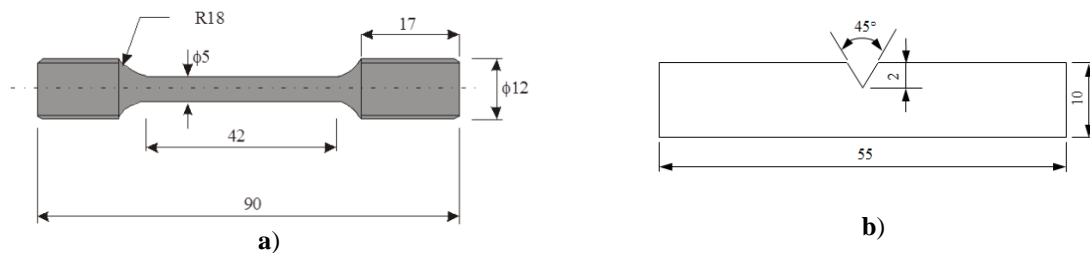
Figure 1: Specimens used in: a) Tensile test. b) Charpy test. All dimensions in mm

If trying to design a structure resistant to fracture, fracture toughness is an important parameter that designers need to account for. On the basis of Charpy V-notch (CVN) impact energy, obtained by simple Charpy test using standardized specimen, Fig. 1, correlation with fracture toughness can be made, e.g. with Roberts-Newton formula independent of CVN energy range and temperature level [15]:

$$K_{Ic} = 8.47(\text{CVN})^{0.63} . \tag{1}$$

Crack propagation resistance is usually described by one or more fracture mechanics parameters obtained by experimental research, e.g. crack tip opening displacement (*CTOD*), *J*-integral or stress intensity factor (*K*). *J*-integral is a suitable parameter when observing ductile fracture in metals materials. Rice [16] introduced *J*-integral as an integral encircled around the crack tip, path-independent as long as the stress is a function of strain alone and provided the crack tip is the only singularity within the contour. It can be considered equally energy release rate parameter and stress intensity parameter. In a two-dimensional form, it can be written as:

$$J = \int_{\Gamma} \left(w\mathrm{d}y - T_i \frac{\partial u_i}{\partial x} \mathrm{d}s \right).$$

(2)

Here, $T_i = \sigma_{ij}n_j$ are components of the traction vector, u_i are components of displacement vector, ds is an incremental length along the integral contour Γ. When contour Γ shrinks to the crack tip, J_{Ic} parameter can be derived, describing fracture resistance of material, i.e. required energy for crack growth per unit length. Further, strain energy density w is:

$$w = \int \sigma_{ij} \mathrm{d}\varepsilon_{ij} ,$$

(3)

where ε_{ij} is the sum of elastic and plastic strains at a specific point. When dealing with a growing crack, J values can be correlated to extension of a crack (Δa) giving resistance curve (R). For this, standardized experimental procedures are usually used but in some cases, they can be accompanied or even substituted by modern numerical methods, e.g. finite element (FE) method. For instance, accuracy check was performed to compare J-integral values obtained by experiment, two-dimensional and three-dimensional FE analysis and EPRI method [17]. Mode I fracture is studied in a compact tensile (CT) specimen using FEM in order reveal multiscale effects [18]. Also, numerically determined plastic geometry factors are used to calculate J-integral from the load vs. crack mouth opening displacement or load-line displacement curve in the J-R curve test.

In this paper, experimental single specimen test method [19] following elastic unloading compliance technique is numerically simulated in order to predict fracture behavior of considered steels. Numerical stress analysis is performed on a two-dimensional FE model of single edge notched bend (SENB) specimen, Fig. 2. Three initial relative crack length a/W (W = 50 mm) ratios are taken, 0.25, 0.5 and 0.75. Material behavior is considered to be multilinear isotropic hardening. Specimen model is discretized with 8-node isoparamateric quadrilateral elements. FE mesh is refined around the crack tip because high deformation gradients occur in the yielding region. Quasi-static load was imposed on specimen in order to simulate compliance procedure of single specimen test method. Only half of the specimen needs to be modelled due to symmetry. To simulate crack propagation node releasing technique was used.
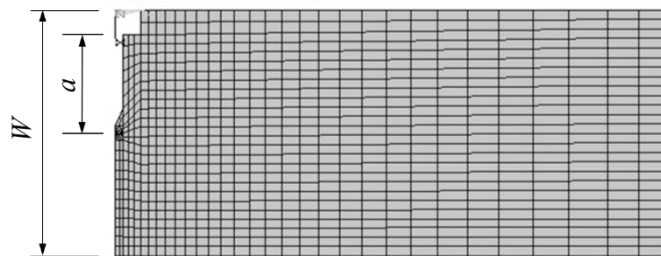
Figure 2: FE model of SENB specimen

Stress analysis results extracted from integration points of finite elements enclosing crack tip are used to evaluate J values in integration points by Eq. 4 [20]. Summing them along a path Γ that encloses crack tip gives total value of J that can be correlated to crack extension values.

$$J = \sum_{p=1}^{np} G_p I_p \left(\xi_p, \eta_p \right), \tag{4}$$

Here, G_p represents Gauss weighting factor, np stands for the number of integration points and I_p is the integrand evaluated at each Gauss point p:

$$
\begin{aligned}
I_p = & \left\{ \frac{1}{2} \left[\sigma_{xx} \frac{\partial u_x}{\partial x} + \sigma_{xy} \left(\frac{\partial u_x}{\partial y} + \frac{\partial u_y}{\partial x} \right) \frac{\partial u_x}{\partial x} + \sigma_{yy} \frac{\partial u_y}{\partial y} \right] \frac{\partial y}{\partial \eta} \right. \\
& \left. - \left[\left(\sigma_{xx} n_1 + \sigma_{xy} n_2 \right) \frac{\partial u_x}{\partial x} + \left(\sigma_{xy} n_1 + \sigma_{yy} n_2 \right) \frac{\partial u_y}{\partial x} \right] \sqrt{ \left(\frac{\partial x}{\partial \eta} \right)^2 + \left(\frac{\partial y}{\partial \eta} \right)^2 } \right\}_g .
\end{aligned}
\tag{5}
$$

In order to account for possible minor variation of J values in numerical analysis, three different paths around the crack tip are taken in each example and their average value is taken as final. The procedure is verified on steels 1.4021 and 1.4057 [21], comparing available experimental results with obtained numerical values.

3   RESULTS

3.1 Experimentally determined material properties

Experimentally determined engineering stress-strain (σ - ε) diagrams for three steels are given in Fig. 3. Experimentally determined Charpy V-notch energy is presented in Table 1, along with fracture toughness obtained by Eq. 1. In addition to that, yield strength (σ_{YS}), tensile strength (σ_{TS}) and Young's modulus (E) values are given in Table 1, also.
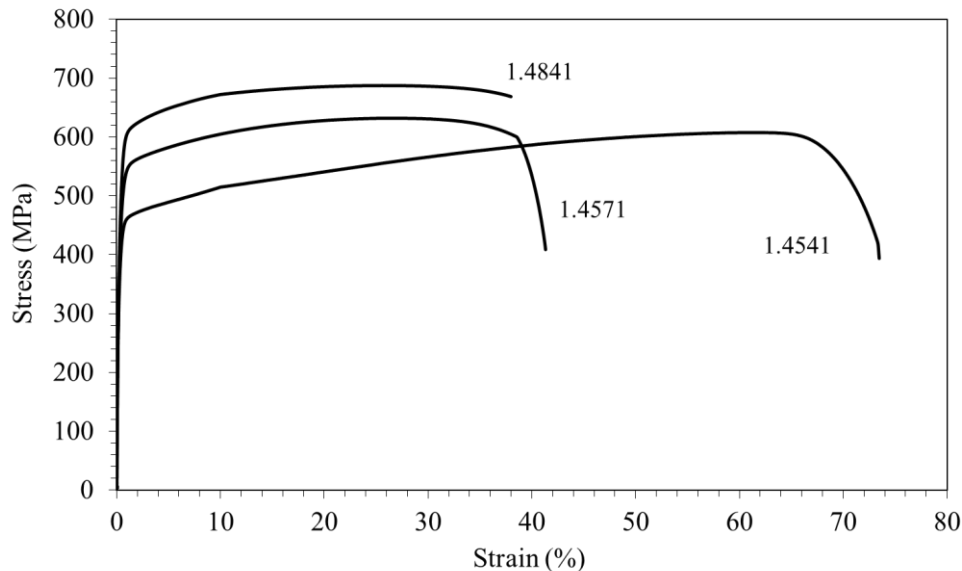
Figure 3: Steels 1.4841, 1.4571, 1.4541: uniaxial engineering stress-strain diagrams

5

Table 1: Yield strength (σ_{YS}), tensile strength (σ_{TS}), Young's modulus (E), Charpy V-notch impact energy (CVN) energy and fracture toughness (K_{Ic}) of considered stainless steels

Material	σ_{YS} [MPa]	σ_{TS} [MPa]	E [GPa]	CVN [J]	K_{Ic} [MPa·m$^{0.5}$]
AISI 321[13]	390	607	224	170	215.3
AISI 316Ti	458	632	186	158	205.6
AISI 314	498	688	220	312	315.6

3.2 Numerically predicted fracture behaviour

Fig. 4, 5 and 6 show final J values for steels 1.4541, 1.4571, 1.4841 taken as a measure of crack driving force for different initial crack lengths (a/W) and according to crack propagation (Δa).
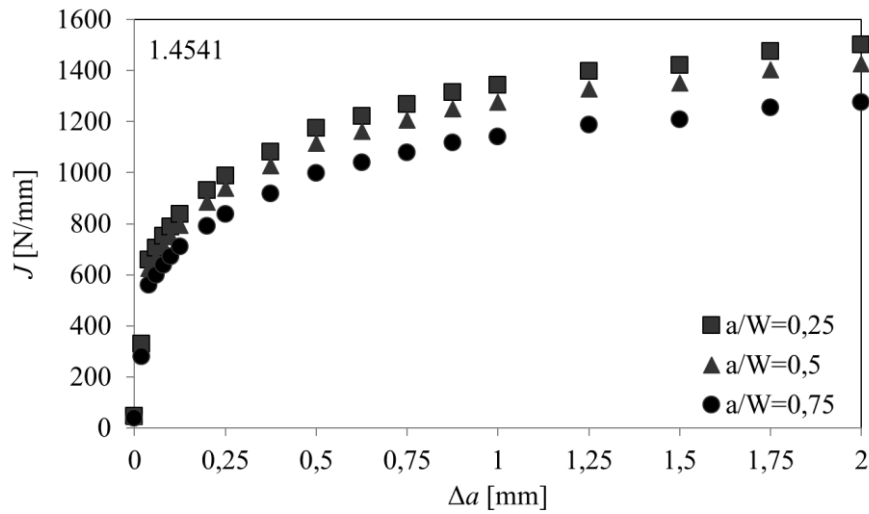
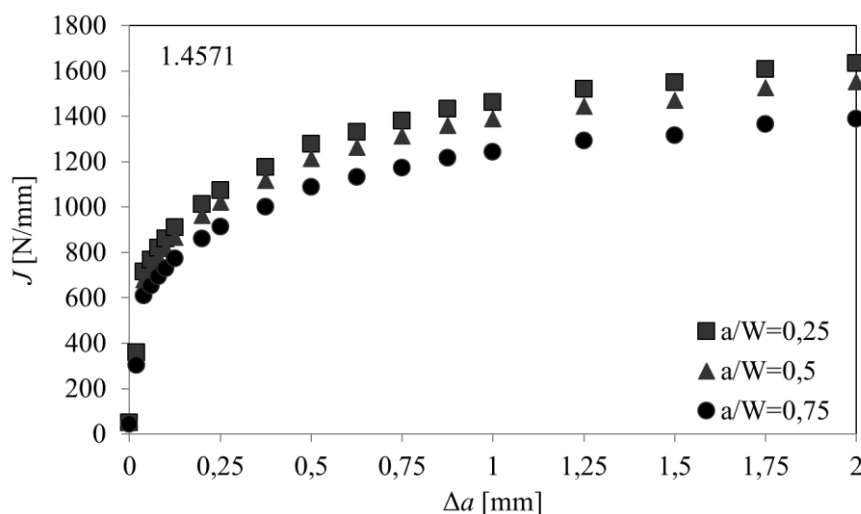**Figure 4**: J-integral values obtained numerically for steel

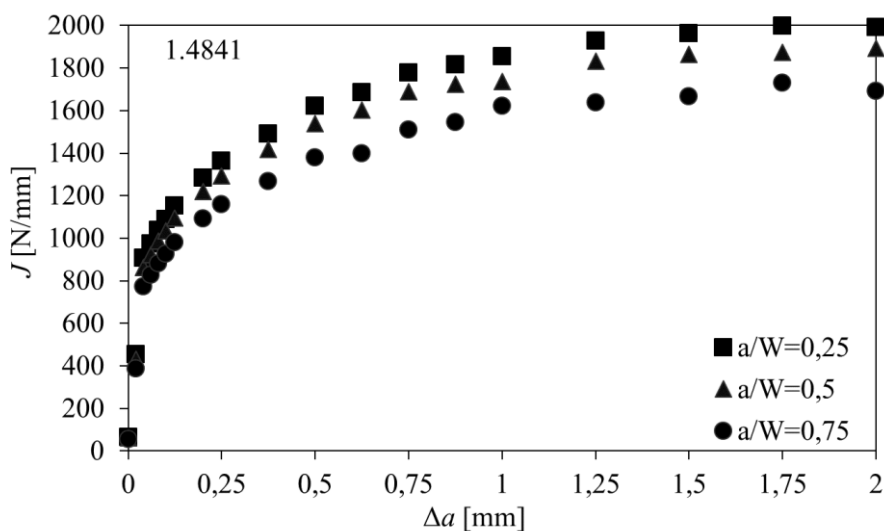**Figure 5**: *J*-integral values obtained numerically for steel

Figure 6: *J*-integral values obtained numerically for steel

4 DISCUSSION

Comparing the chemical composition of three considered steels, it can be noted that 1.4541 and 1.4571 have somewhat similar composition, except of the titanium and molybdenum percentage that are in favour of 1.4571. Steel 1.4841 is quite different in terms of chemical composition, especially regarding significantly higher values of silicon, chromium and nickel when comparing to 1.4541 and 1.4571.

Having this composition differences in mind, it was expected that 1.4841 has the highest yield and ultimate tensile strength of three compared steels. This expectation is proved by performed tensile tests, Table 1. As for the experimentally measured Charpy impact energy and derived fracture toughness, it can be noted that 1.4841 has significantly higher both values when

comparing it to 1.4541 and 1.4571.

Fracture behaviour of steels 1.4541, 1.4571 and 1.4841 can be predicted based on the numerical analysis results shown in Fig. 4, 5 and 6 where J-integral values are used as a measure of crack driving force. Observing diagrams, it is obvious that steel 1.4841 has higher values of J-integral than the other two, making it more adequate to structures that need less susceptibility to fracture. Numerically predicted values comply with experimentally determined CVN and calculated K_{Ic}.

Predicted difference in numerically obtained J values and consequential difference in resistance to crack extension of steels 1.4541, 1.4571 and 1.4841 can be contributed to different composition and properties of three steels. Higher percentage of nickel and chromium, as previously mentioned in this paragraph, in steel 1.4841 can add to noted behaviour. Further, observing Fig. 4, 5 and 6, it can be noted that lower a/W ratios correspond to higher J values and opposite. J-integrals for $a/W = 0,25$ and $0,5$ tend to be close in values, while the ones for $a/W = 0,75$ differs greatly. As for the crack geometry, a/W ratios were kept equal for all steels minimizing the influence of geometry on difference in J values.

5 CONCLUSION

This paper provides overview of experimentally and numerically determined properties and characteristics of three austenitic chromium-nickel alloys, 1.4541, 1.4571 and 1.4841. Standardized tensile test provided values of ultimate tensile strength and yield strength while Charpy test provided impact energy values and fracture toughness. Numerically, fracture behavior of the three mentioned steels is described using J-integral as a prediction of crack driving force. Results obtained experimentally and numerically are compared and discussed. 1.4841 tends to prove optimal choice when there is a need for a stainless steel with higher values of ultimate tensile strength and yield strength along with fracture resistance. However, specific benefits of the other two steels should not be neglected in specific applications when there is a need for resistance to high temperatures or to creep effect. Results of the investigation presented in this paper can be used in the design process to avoid failures of constructions and structures.

REFERENCES

[1] Brnić, J. *Analysis of Engineering Structures and Material Behaviour*, John Wiley & Sons, 1st ed., (2018).

[2] Sanchez, J., Galao, O., Torres, J., Fullea, J., Andrade, C., Garcia, J.C., Ruesga, J., Cano, P. 40 years old LNG stainless steel pipeline: Characterization and mechanical behaviour. *Eng Fail Anal* (2017) **79**:876-888.

[3] Suzuki, R., Matsubara, M., Yanagihara, S., Morijiri, M., Omori, A., Wakai, T. Collapse Evaluation of Double Notched Stainless Pipes Subjected to Combined Tension and Bending. *Proce Mat Sci* (2016) **12**:24-29.

[4] He, J., Sandström, R. Basic modelling of creep rupture in austenitic stainless steels. *Theoret Appl Fract Mech* (2017) **89**:39-146.

[5] Poza, P., Múnez, C.J., Rodríguez, R., Rodríguez, J. Plastic collapse of a stainless steel pressurized tube. *Eng Fail Anal* (2010) 17(2):530-536.

[6] Noury, P., Eriksson, K. Failures of high strength stainless steel bridge roller bearings: A review. *Eng Fract Mech* (2017) **180**:315-329.

[7] Corbett, R.A., Sherman, F.M. Corrosion of a stainless steel handrail. *J Fail Anal Prev* (2005) **5(1)**:8-12.

[8] Jha, A.K., Sreekumar, K. Failure Analysis of Stainless Steel Pipeline Used in Propulsion Engine Test Facility. *J Fail Anal Prev* (2009) **9(3)**:222-226.

[9] Franulovic, M., Basan, R., Prebil, I., Trajkovski, A., Marohnić, T. Materials characterization – From metals to soft tissues. *Materials Discovery* (2017) **7**:1-7.

[10] Piekarska, W., Rek, K. Numerical Analysis and Experimental Research on Deformation of Flat Made of TIG Welded 0H18N9 Steel, *Proc Eng* (2017) **177**:182-187.

[11] Vukelic, G., Brnic, J. Numerical Prediction of Fracture Behavior for Austenitic and Martensitic Stainless Steels. *Int J Appl Mech* (2017) **9(4)**:1750052.

[12] Liu, C., He, A., Qiang, Y., Guo, D., Shao, J. Effect of Internal Stress of Incoming Strip on Hot Rolling Deformation Based on Finite Element and Infinite Element Coupling Method. *Metals* (2018) **8**:92.

[13] Brnic, J., Turkalj, G., Canadija, M., Lanc, D., Krscanski, S., Brcic, M., Li, Q., Niu, J. Mechanical properties, short time creep and fatigue of an austenitic steel, *Materials*, (2016) **9(4)**:298-1-298-19.

[14] Annual Book of ASTM Standards, Metal Test Methods and Analytical Procedures. ASTM International: Baltimore, USA, 2005, Vol. 03.01.

[15] Roberts, R., Newton, C. Interpretive Report on Small Scale Test Correlations with KIc Data. *Welding Research Council Bulletin*, (1981) **265**:1–16.

[16] Rice, J.R. A Path Independent Integral and the Approximate Analysis of Strain Concentration by Notches and Cracks. *J Appl Mech* (1968) **35**:379-386.

[17] Qiao, D., Changyu, Z., Jian P., Xiaohua H. Experiment, Finite Element Analysis and EPRI Solution for J-Integral of Commercially Pure Titanium. *Rare Metal Mater Eng* (2014) 42(2):257-63.

[18] Saxena S., Ramakrishnan N. A comparison of micro, meso and macroscale FEM analysis of ductile fracture in a CT specimen (mode I). *Computational Materials Science*, (2014) **39(1)**:1-7.

[19] Huang Y., Zhou W., Yan Z. Evaluation of plastic geometry factors for SE(B) specimens based on three-dimensional finite element analyses. *Int J Press Vessel Pip*, (2014) **123-124**:99-110.

[20] Standard test method for measurement of fracture toughness E1820, ASTM, Baltimore, USA, 2005.

[21] De Araujo T.D., Roehl D., Martha L.F. An Adaptive Strategy for Elastic-Plastic Analysis of Structures with Cracks, *J Brazil Soc Mech Sci Eng*, (2008) **30(4)**:341-350.